Rothamsted Repository Download

A - Papers appearing in refereed journals

The publisher's version can be accessed at:

- https://doi.org/10.1016/j.scitotenv.2023.162332
- https://www.sciencedirect.com/science/article/pii/S0048969723009488?via%3Dihub

The output can be accessed at: https://repository.rothamsted.ac.uk/item/98v71/use-of-a-submersible-spectrophotometer-probe-to-fingerprint-spatial-suspended-sediment-sources-at-catchment-scale.

Use of a submersible spectrophotometer probe to fingerprint spatial suspended sediment sources at catchment scale

Niels F. Lake [a,b,*], Núria Martínez-Carreras [a], Jean François Iffly [a], Peter J. Shaw [b], Adrian L. Collins [c]

[a] Environmental Research and Innovation (ERIN) Department, Luxembourg Institute of Science and Technology (LIST), 41 rue du Brill, L-4422 Belvaux, Luxembourg
[b] Centre for Environmental Science, School of Geography and Environmental Science, University of Southampton, Highfield, Southampton, Hampshire SO17 1BJ, United Kingdom
[c] Net Zero and Resilient Farming, Rothamsted Research, North Wyke, Okehampton EX20 2SB, United Kingdom

HIGHLIGHTS

- A method is presented using UV-VIS absorbance for sediment fingerprinting.
- Fingerprints were measured on water samples using a submersible spectrophotometer.
- Confluence-based sampling allowed to fingerprint spatial source contributions.
- Modelled source contributions evaluated against a sediment budget deviated by 18 %.
- The method shows potential for in-stream, high frequency sediment fingerprinting.

GRAPHICAL ABSTRACT
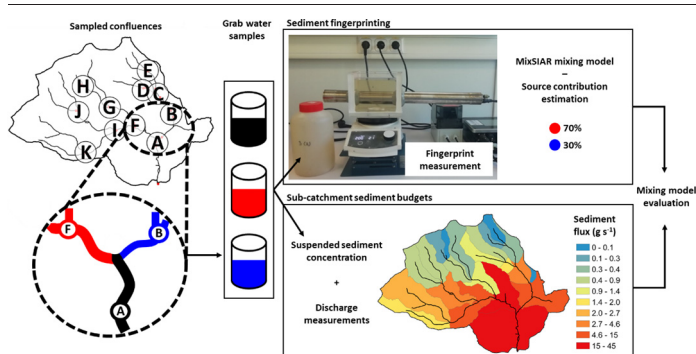
ARTICLE INFO

ABSTRACT

Sediment fingerprinting is used to identify catchment sediment sources. Traditionally, it has been based on the collection and analysis of potential soil sources and target sediment. Differences between soil source properties (i.e., fingerprints) are then used to discriminate between sources, allowing the quantification of the relative source contributions to the target sediment. The traditional approach generally requires substantial resources for sampling and fingerprint analysis, when using conventional laboratory procedures. In pursuit of reducing the resources required, several new fingerprints have been tested and applied. However, despite the lower resource demands for analysis, most recently proposed fingerprints still require resource intensive sampling and laboratory analysis. Against this background, this study describes the use of UV-VIS absorbance spectra for sediment fingerprinting, which can be directly measured by submersible spectrophotometers on water samples in a rapid and non-destructive manner. To test the use of absorbance to estimate spatial source contributions to the target suspended sediment (SS), water samples were collected from a series of confluences during three sampling campaigns in which a confluence-based approach to source fingerprinting was undertaken. Water samples were measured in the laboratory and, after compensation for absorbance influenced by dissolved components and SS concentration, absorbance readings were used in combination with the MixSIAR Bayesian mixing model to quantify spatial source contributions. The contributions were compared with the sediment budget, to evaluate the potential use of absorbance for sediment fingerprinting at catchment scale. Overall deviations between the spatial source contributions using source fingerprinting and sediment budgeting were 18 % for all confluences (n = 11), for all events (n = 3). However, some confluences showed much higher deviations (up to 52 %), indicating the need for careful evaluation of the results using the spectrophotometer probe. Overall, this study shows the potential of using absorbance, directly obtained from grab water samples, for sediment fingerprinting in natural environments.

* Correspondence to: N.F. Lake, Environmental Research and Innovation (ERIN) Department, Luxembourg Institute of Science and Technology (LIST), 41 rue du Brill, L-4422 Belvaux, Luxembourg
  E-mail addresses: niels-lake3@hotmail.com (N.F. Lake), nuria.martinez@list.lu (N. Martínez-Carreras).

1. Introduction

Sediment fingerprinting is commonly used to estimate suspended sediment (SS) sources (see e.g., reviews by Collins et al., 2017, 2020). It is increasingly used to assemble much needed information for targeting best management interventions for addressing issues resulting from excessive SS inputs, such as reduced light penetration in the water column (Owens et al., 2005) and increased siltation (Nones, 2019; Owens et al., 2010). Identifying SS sources is especially important in the pursuit of improving the ecological status of surface waters, as dictated by legislation such as the European Water Framework Directive (WFD; 2000/60/EC, 2000). The need to take action is becoming even more crucial in the context of global change, as human activities and related changes to land use are accelerating soil erosion and concomitant sediment delivery at global scale (Borrelli et al., 2017).

The sediment fingerprinting approach is based on the identification and collection of samples of potential sediment sources, which, together with target SS samples, are analysed in the laboratory. Differences between the properties of the sampled sources, i.e., their fingerprints, are then used to estimate the relative contribution of each source to the target SS (e.g., Collins et al., 2020). However, collection of representative source material and SS sampling, and conventional laboratory analyses of commonly-used fingerprints generally require high workloads and generate substantive analytical costs (Collins et al., 2020; Evrard et al., 2022), therefore limiting their application beyond academic research (Pulley and Collins, 2021). There is thus a need for easier-to-measure fingerprints in combination with simplified sampling procedures to allow for a wider uptake of the approach (Pulley and Collins, 2021).

To this end, fingerprinting procedures based on cheaper and easier measurements have been developed and tested. These include, for instance, the use of conventional document scanners (e.g., Pulley and Collins, 2022; Pulley and Rowntree, 2016) to measure colour fingerprints, and spectrometers from which both geochemical fingerprints (e.g., Cooper et al., 2015; Cooper et al., 2014; Martínez-Carreras et al., 2010a) and colour (e.g., Legout et al., 2013; Martínez-Carreras et al., 2010b) have been derived. These less onerous techniques offer the potential to increase the number of observations to subsequently inform how SS sources change at finer temporal and spatial scales (e.g., Cooper et al., 2015; Cooper et al., 2014). High frequency temporal data might facilitate a better and fuller understanding of which SS sources contribute at which time and in what proportions to the target SS, as sediment delivery from sources to streams is complex, involving different processes at multiple spatial and temporal scales (Fryirs, 2012).

While some techniques allow for fingerprints to be measured with relative ease, the need for SS sampling, preparation and laboratory analysis remains. In an attempt to overcome such resource demands, Lake et al. (2022a) tested the novel use of a UV-VIS spectrophotometer sensor for sediment fingerprinting purposes. Artificially created mixtures were used, consisting of soil source samples with clear contrasts in colour and geochemistry, i.e., differences that were expected to influence the absorbance spectra at different wavelengths (i.e., fingerprints) (Lake et al., 2022a). Known soil source contributions for each mixture were used to evaluate the mixing model results (when using the MixSIAR Bayesian mixing model) (Stock et al., 2018; Stock and Semmens, 2016). Evaluation indicated satisfactory results for the un-mixing of mixtures consisting of two and three different soil samples (with respective mean absolute errors between known inputs and model results of 15 % and 13 % respectively); but the un-mixing results for mixtures consisting of four soil samples were slightly less robust (with respective mean absolute errors of 17 %). Analysis showed that SS concentration, particle size and the water environment influenced the absorbance data. During these initial tests, only controlled experiments in a laboratory tank (with 40 L of water) were conducted. As the submersible spectrophotometer used was designed to conduct in-stream measurements, it was proposed that the spectrophotometer probe could be used in field studies to fingerprint SS source contributions at high temporal resolution. Contrary to other fingerprinting methods that require

laboratory analysis, this approach could decrease the interval between measurements (e.g., measurement interval of minutes) without adding to resource needs for sampling and analysis (i.e., direct in-stream fingerprint measurements). Insights into temporal changes in SS source contributions and, specifically, a more detailed investigation into the activation of specific sources at different times might thus be improved (e.g., Cooper et al., 2015; Navratil et al., 2012; Vercruysse et al., 2017). This information is essential to understand the hydro-sedimentary dynamics of a catchment (i.e., changes over short temporal scales), and important if targeted sediment control strategies are to be implemented (e.g., Vercruysse et al., 2017).

Despite the reliable laboratory performance, it remains to be assessed how well the approach presented by Lake et al. (2022a) performs with 'real world' samples. Fingerprints do not always allow for accurate catchment source apportionment, even if they perform well in laboratory setting (Batista et al., 2022). The present study therefore tests if absorbance, measured on grab water samples and using a confluence-based sampling strategy, can be used to determine the relative contributions of individual spatial sediment sources. This sampling strategy considers in-stream SS from upstream tributaries as the spatial sources, and in-stream SS from the downstream channel as the target SS (e.g., Collins et al., 1997; Collins et al., 1996; Klages and Hsieh, 1975). This procedure circumvents challenges in determining which soil sources are contributing to target SS by using tributary SS samples to represent the spatially-integrated fingerprints of sub-catchments. Furthermore, with the confluence-based approach, difficulties in determining which particle size fractions are transported from potential soil sources (i.e., source types rather than spatial sources) to the stream are circumvented by only considering those fractions already delivered to the tributary catchment streams (Laceby et al., 2017). This facet is important since sediment fingerprints often vary with particle size (Collins et al., 2017; Laceby et al., 2017): particle size directly influences absorbance values (Lake et al., 2022a; Sehgal et al., 2022).

Building on the work of Lake et al. (2022a) and taking into account the aforementioned limitations regarding the resource needs in sediment fingerprinting, this study aims to obtain rapid absorbance measurements at the 200–730 nm wavelength range (i.e., sediment fingerprints) directly measured on grab water samples using a submersible UV-VIS spectrophotometer probe. These absorbance output readings will then be used directly to estimate spatial suspended sediment sources at catchment scale. To this end, we first evaluated the potential of the selected catchment to discriminate between spatial SS sources by investigating (i) differences in absorbance between source streams, and (ii) how absorbance patterns in same sampling sites compared during different campaigns, to investigate temporal (in)consistency in spatial SS source fingerprints. Secondly, modelled spatial source contributions, using the MixSIAR Bayesian mixing model (Stock et al., 2018; Stock and Semmens, 2016), were then compared with the calculated sediment budget, based on SS concentration and discharge measurements, to evaluate model performance.

2. Materials and methods

Manual grab water samples were collected during storm runoff events at a series of confluences, following a confluence-based sampling strategy. The samples were analysed using a UV-VIS spectrophotometer installed in a custom-made laboratory test chamber. The absorbance spectra of the SS spatial source samples and downstream target SS sample were then used to estimate the relative contributions of each source using a Bayesian mixing model.

2.1. Sampling sites

Sampling was performed in the Roudbach catchment (44 km² at Platen), located in the western part of Luxembourg (Fig. 1). Land use in the catchment consists of forest, grassland and cultivated land. Lithology is characterised by schist, slates and phyllites bedrock in the northern part, and by red sandstone ("Buntsandstein") and marls in the middle and

southern parts. Altitudes range between 553 m and 260 m above sea level. Land use, lithology and elevation data is made available by the 'Administration du Cadastre et de la Topographie' (ACT). The climate is semi-oceanic, with monthly maximum mean temperatures varying between 0 °C in January and 18 °C in July, and a long term average annual precipitation of 845 mm (1954–1996; Pfister et al., 2005).

At each confluence (n = 11), manual grab water samples were collected at three sites: at the two upstream SS source sites (between 20 and 10 m upstream of the confluence), and at the downstream target SS site (between 10 and 20 m downstream of the confluence) (Fig. 2). At each sampling site (n = 33), a 2-L grab sample was collected during three storm runoff events: campaign 1 was carried out on 03/11/2021, campaign 2 on 04/01/2022 and campaign 3 on 16/02/2022. Samples were stored in a dark, cold room (4–5 °C) and analysed in the following 2–5 days. Precipitation records from the weather station at Reichlange (see Fig. 1b,c) were made available by the 'Administration de la Gestion de l'Eau' (AGE).

2.2. Laboratory analyses

A sub-sample of each grab water sample was filtered to determine its suspended sediment concentration (SSC) by filtering a known volume through pre-weighed 1.2 μm pore size Whatman GF/C glass fibre filters. Filters were dried at 105 °C and weighed, and after filtration, again dried at 105 °C and weighed. The filtrate water for each sample was collected and stored for 1–3 days. Measured SSCs for all sampling sites, for the three campaigns, are shown in Table 1.

Grab samples were analysed using a S::can spectro::lyser™ submersible spectrophotometer probe (Scan Messtechnik GmbH, Vienna, Austria), installed in a custom-made laboratory test chamber (Fig. 3a). The spectrophotometer records on the absorbance over the UV-VIS wavelength range (200–730 nm) at 2.5 nm intervals by measuring the transmittance of a light beam (i.e., xenon-flash light) through the water sample. The spectrophotometer, with a 15 mm optical path length, was installed horizontally in the test chamber (inner dimensions 14x10x10 cm) to avoid potential settling of SS particles on the measurement window. A magnetic stirrer was used to make sure all particles were kept in suspension (visually checked for all samples tested). Grab water samples were shaken well by hand, and an aliquot of ~1.2 L was poured into the test chamber. After allowing homogenisation within the test chamber for 2-min, the spectrophotometer measured for 6-min at 2-min intervals (n = 4). After each grab sample, the test chamber was rinsed with milli-Q water and dried. Absorbance at each measured wavelength was divided by measured SSCs to eliminate the effect of SSC on absorbance (see Lake et al., 2022a).

The absorbance of the grab water samples after filtration was measured using the multifunctional slide provided by the manufacturer (Scan Messtechnik GmbH, Vienna, Austria; Fig. 3b). Measurements were made over a 6-min timeframe, at 2-min intervals (n = 4). After each sample, the slide was rinsed with milli-Q water and dried. Grab sample absorbance measurements were then compensated by subtracting the filtered water
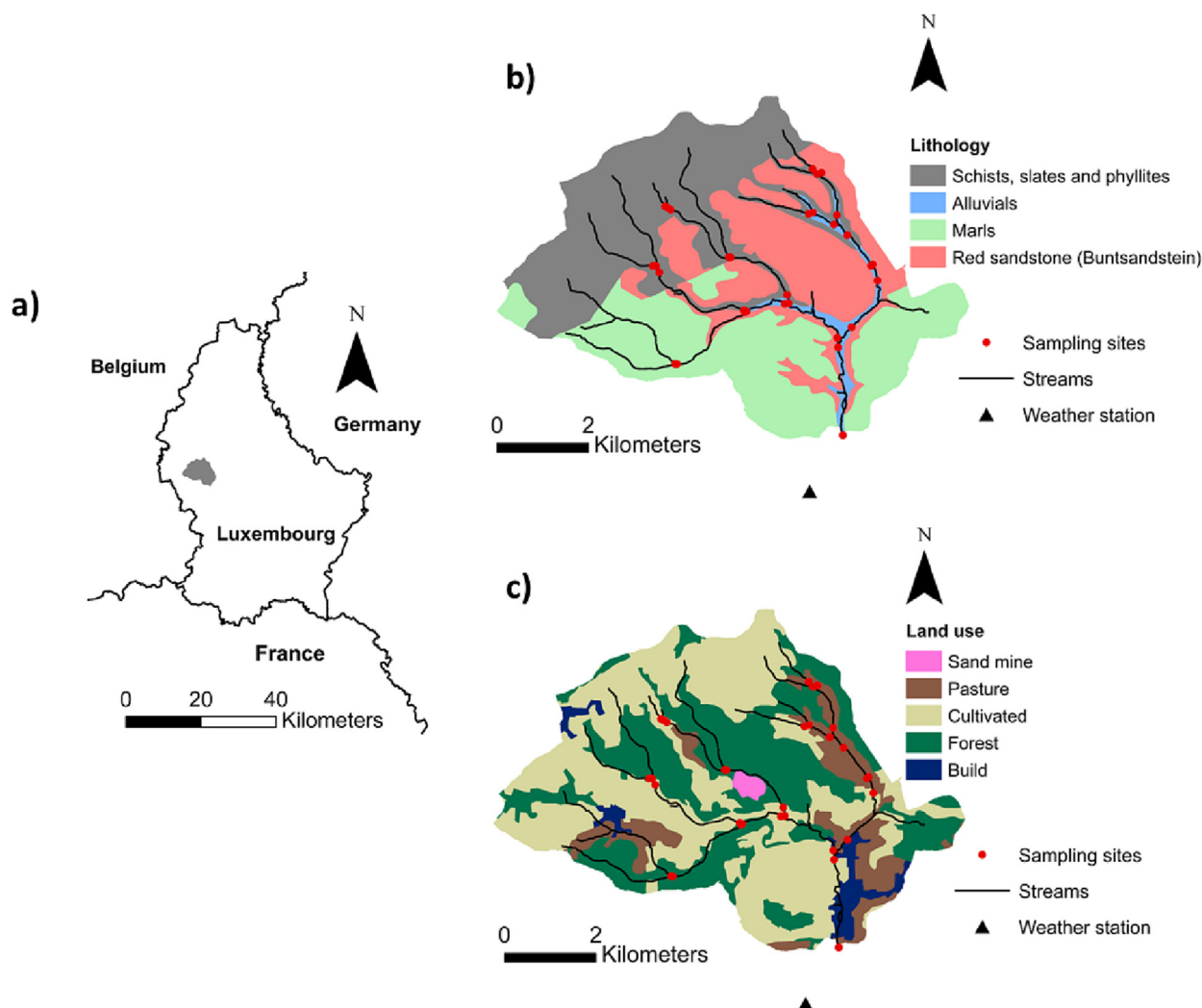
Fig. 1. Location of the Roudbach catchment in Luxembourg (a), catchment lithology (b) and land use (c).
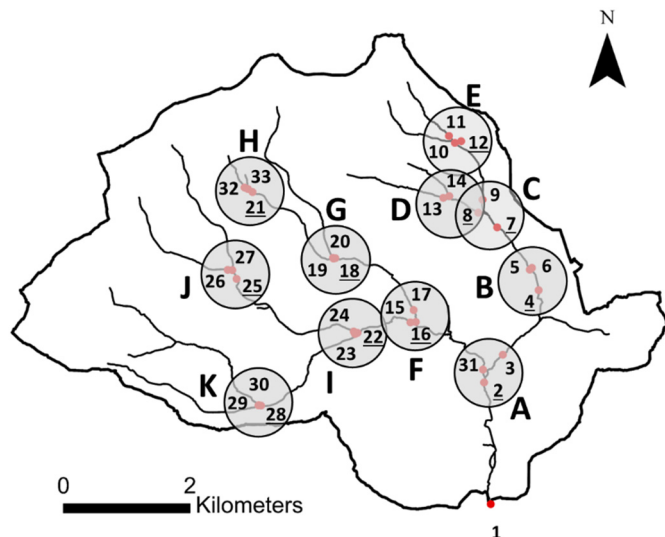
Fig. 2. Sampling sites (numbers 1–33) within the Roudbach catchment. Each circle represents a confluence (letters A-K) enclosing the two upstream spatial source sampling sites and the downstream target suspended sediment sampling site (underlined number). Sampling site 8 is both a spatial source (confluence C) and target (confluence D) SS sampling site. The catchment outlet is located at sampling site 1.

absorbance spectrum of the corresponding grab sample to eliminate the influence of the dissolved, non-SS components on absorbance spectra. Similarly, Lake et al. (2022a) compensated their absorbance measurements by subtracting the absorbance of the deionized water used during the experiments.

2.3. Discharge measurements

At five sampling sites (sites 1, 3, 17, 23, 31; Fig. 2), the water level was measured continuously at 15-min intervals during the period 22/10/2021–22/03/2022 using ISCO 4120 pressure probes. Discharge time series were created by means of a rating curve between water level and discharge. Water levels and discharges were measured in parallel during the days of the sampling campaigns (n = 3), at different times during the day (n = 4) to cover relatively higher and lower discharges.

Specific discharge was calculated for each site with available discharge measurements The surface catchment area (Table S3) contributing to discharge at each site was calculated using ArcMap 10.5 (ESRI, Redlands, CA). Specific discharge data and computed catchment areas were then used to estimate discharge at the ungauged sampling sites using the drainage area method (e.g., Emerson et al., 2005). Estimated discharges for all sampling sites, for the three campaigns, are shown in Table 1.

2.4. Evaluating the use of absorbance spectra for sediment source fingerprinting

The following analyses were carried out to evaluate the potential use of absorbance to fingerprint spatial SS sources under field conditions: analysis of the differences between spatial source absorbance values and patterns therein (Section 2.4.1); evaluation of modelled spatial source contributions against the estimated sediment budgets (Section 2.4.2), and; comparison of model results when using different wavelength selection procedures, to evaluate the possibility of omitting the need for absorbance compensation and to eventually reduce un-mixing calculation times (Section 2.4.3).

2.4.1. Absorbance patterns

Absorbance patterns were analysed in two different ways. First, average absorbance over the full range of wavelengths (200–730 nm) was calculated for each sampling site and compared. Second, for each confluence, mean absorbance differences between the two sources were calculated.

These approaches permit the investigation of (i) differences in mean spatial source absorbances for the same sites during the different sampling campaigns, (ii) differences in mean source absorbances between the spatial sources merging at the confluences, and (iii) whether these differences influenced deviations between the modelled spatial source contributions and the sediment budget estimations (Section 2.4.2).

2.4.2. Sediment and water budgets

Measured SSCs (Section 2.2) and discharge data (at gauged and ungauged sites; Section 2.3) were used to calculate the relative contribution of SS and water from the upstream tributaries to the downstream sampling sites (Table 1). The sediment budget was then used to evaluate the un-mixing modelling predictions of spatial source contributions using the absorbance data as a fingerprint (Section 2.4.3).

2.4.3. Un-mixing modelling

The MixSIAR model (Stock and Semmens, 2016; Stock et al., 2018) was used to un-mix the downstream target SS into the spatial source contributions using absorbance data. Model runs were executed for all sampled confluences, including when absorbance values from the target SS were outside the range of absorbance values of the spatial source streams. For all model runs, the Markov Chain Monte Carlo parameters were set as long (chain length = 300.000, burn = 200.000, thin = 100, chains = 3). Model convergence was evaluated using the Gelman-Rubin diagnostic (variables <1.1). For each model run, MixSIAR output predicts a relative average contribution of each source with its corresponding standard deviations. All models were run using the High Performance Computing (HPC) facility at the Luxembourg Institute of Science and Technology (LIST).

The modelling approach applied herein used the wavelengths (with 2.5 nm intervals) in the 200–730 nm range (Lake et al., 2022a) as fingerprints (n = 213). Absorbance data for all grab samples were compensated for: (i) the absorbance of the filtered water to account only for the absorbance influenced by the SS (Section 2.2; Lake et al., 2022a), and; (ii) the measured SSC to eliminate the effect of concentration (Lake et al., 2022a). Modelled spatial source contributions were compared with the sediment budgets.

Two other modelling approaches were tested and reported in this study. These approaches focus on the use of the 390–730 nm wavelength range. This part of the absorbance spectrum, the visible light spectrum, is highly related to turbidity (e.g., Rieger et al., 2004) and is therefore mainly influenced by SS particles. Using only this part of the wavelength range, removes, in principle, the effect of dissolved components that primarily influence wavelengths in the 200–390 nm range (e.g., Byrne et al., 2011; Fig. S2). A modelling approach using only the 390–730 nm wavelengths range should not therefore require compensation for the filtered water to eliminate the influence of dissolved components on the spectra. This approach also reduces computation time due to the lower number of wavelengths (n = 137). Subsequently, so as to further reduce computation times, a second modelling approach was tested using the absorbance measurements in the 390–730 nm range with a lower resolution (absorbance readings at 10 nm intervals; n = 35). This approach maintained the broad patterns of the absorbance data, while reducing the number of input wavelengths considered.

3. Results

3.1. Water and sediment budget

Total precipitation (in Reichlange) for the sampled storm runoff events was 10.9 mm for campaign 1, 47.2 mm for campaign 2, and 18.1 mm for campaign 3. An overview of the precipitation records and measured discharge at the catchment outlet in Platen is provided in Fig. 4. Campaign 1 was conducted during one of the first storm runoff events of the hydrological year, during wetting-up. Campaign 2 took place during a large storm runoff event with much higher discharges than campaigns 1 and 3. Campaign 3 was performed during a storm runoff event of similar magnitude

Table 1

Summary of the hydro-sedimentological data at all sampled spatial source sites for the three sampling campaigns. Data shown are the measured suspended sediment concentrations (SSCs), estimated discharge values, relative source discharge contributions to the downstream target SS site (in %; computed using a mass-balance approach), the estimated sediment flux, and the relative spatial source sediment load contribution at the time of sampling.

Confluence	Campaign	Source sampling site	SSC (mg L⁻¹)	Discharge (m³ s⁻¹)	Discharge (%)	Sediment flux (g s⁻¹)	Sediment load (%)
A	1	31	35.1	0.44	68	15.5	60
		3	49.8	0.21	32	10.3	40
	2	31	683.6	3.32	70	2271	85
		3	281.8	1.43	30	403	15
	3	31	42.2	0.63	70	27	74
		3	35.2	0.27	30	9.7	26
B	1	5	28.0	0.14	98	3.9	99
		6	11.4	0.004	2	0.04	1
	2	5	160.0	0.98	98	156	99
		6	60.7	0.02	2	1.5	1
	3	5	19.9	0.19	98	3.8	99
		6	6.8	0.005	2	0.03	1
C	1	8	66.2	0.07	53	4.5	90
		9	8.3	0.06	47	0.5	10
	2	8	83.0	0.07	15	5.7	5
		9	279.6	0.39	85	108	95
	3	8	22.3	0.09	54	1.9	83
		9	5.9	0.07	46	0.4	17
D	1	13	75.3	0.03	49	2.1	70
		14	30.6	0.03	51	0.9	30
	2	13	78.2	0.19	50	15.2	56
		14	60.4	0.20	50	11.9	44
	3	13	28.4	0.04	49	1.1	55
		14	23.5	0.04	51	0.9	45
E	1	10	–	–	–	–	–
		11	–	–	–	–	–
	2	10	459.8	0.10	47	47.2	67
		11	200.7	0.11	53	22.9	33
	3	10	15.5	0.02	47	0.3	68
		11	6.4	0.02	53	0.14	32
F	1	15	35.1	0.29	71	10.1	78
		17	24.8	0.12	29	2.9	22
	2	15	484.9	2.02	72	978	79
		17	328.4	0.79	28	259	21
	3	15	38.1	0.39	72	15	91
		17	9.0	0.15	28	1.4	9

Confluence	Campaign	Sampling site	SSC (mg L⁻¹)	Discharge (m³ s⁻¹)	Discharge (%)	Sediment flux (g s⁻¹)	Sediment load (%)
G	1	19	8.9	0.05	55	0.4	40
		20	16.6	0.04	45	0.6	60
	2	19	320.2	0.35	55	114	67
		20	196.8	0.29	45	57	33
	3	19	10.9	0.07	55	0.75	66
		20	6.6	0.06	45	0.39	34
H	1	32	–	–	–	–	–
		33	–	–	–	–	–
	2	32	149.7	0.14	70	20.5	75
		33	132.2	0.06	30	7.0	25
	3	32	12.3	0.03	70	0.3	94
		33	2.0	0.01	60	0.02	6
I	1	23	49.5	0.16	57	7.7	76
		24	18.1	0.12	43	2.4	24
	2	23	492.7	1.06	56	520	58
		24	453.8	0.83	44	375	42
	3	23	47.3	0.20	56	9.6	68
		24	28.9	0.16	44	4.6	32
J	1	26	33.3	0.04	51	1.5	60
		27	23.6	0.04	49	1.0	40
	2	26	369.2	0.28	51	104	60
		27	256.7	0.27	49	68	40
	3	26	11.2	0.06	51	0.6	50
		27	11.3	0.05	49	0.6	50
K	1	29	43.3	0.04	29	1.7	36
		30	31.2	0.10	71	3.0	64
	2	29	133.3	0.24	29	33	9
		30	567.5	0.61	71	344	91
	3	29	41.7	0.05	29	2.0	43
		30	22.5	0.12	71	2.7	57

Fig. 3. Photograph of the self-made test chamber with the spectrophotometer probe and the magnetic stirrer during the measurements of the grab samples (a). Photograph of the spectrophotometer probe with the multifunctional slide during the measurements of the filtered water samples (b).

to campaign 1, though with the catchment being in a wetted-up state before the start of the event.

Table 1 presents estimated discharges, measured SSCs and estimated SS fluxes plus the relative source contributions of discharge and SS at the time of sampling. The relative contribution of discharge delivered by each source was mostly stable during the three sampling campaigns at most confluences, with absolute deviations <2 %. There was, however, a clear exception observed in the case of confluence C, wherein campaign 2 the relative discharge deviated by 38 % and 39 % compared with campaigns 1 and 3, respectively. This deviation was also apparent in the relative contribution of SS loads. Site 8 was the dominant contributing SS source in confluence C (Fig. 2) during campaign 1 and 3 (90 and 83 %, respectively), while its contribution was much smaller (5 %) during campaign 2. The relative contribution of SS loads to downstream sites showed overall higher variability than discharge, for all three campaigns. Sources that dominated in terms of discharge also dominated in terms of the SS load. However, SS load relative contributions showed higher variability, with for instance confluence K showing a constant contribution from site 30 in terms of discharge (~71 %) for all three campaigns, while the corresponding SS load contributions were 64, 91 and 57 % for campaigns 1, 2 and 3, respectively.

In Fig. 5, a spatial overview of the SS fluxes within the catchment is shown for the three campaigns. At the downstream confluence (confluence A; Fig. 2), most SS originated from the western tributary (contributing to sampling site 31). Here, during all three campaigns, the highest SS fluxes were measured in the southwestern streams (corresponding to sampling sites 15, 23 and 24; Fig. 2). In the eastern tributary (contributing to sampling site 3), most of the SS came from the southern areas, with the northern streams showing relatively lower sediment fluxes. As observed in the eastern branch of the catchment, most northern streams in the western branch showed as well relatively low SS fluxes for all three sampling campaigns.

3.2. Absorbance patterns

Average absorbance (per unit SS) for the same sites (Fig. 6), measured during the three sampling campaigns, showed pronounced variability. The sites sampled during campaign 3 generally had the highest average absorbance (except for sites 6 and 14 where highest average absorbance was measured during campaign 2). Average absorbance was lower during campaign 2 than during campaigns 1 and 3 for most of the sites located on the western side of the catchment (sites 15–33). Exceptions in this regard were sites 18 and 20, where the average absorbance was highest for campaign 2 (by 18 and 33 % respectively). For the sampling sites on the eastern side of the catchment (sites 1–14), the lowest absorbances were measured for either campaign 1 or 2, with the lowest average absorbances measured during campaign 1 at sampling sites 6, 9, 11 and 12. Site 13 showed the lowest variability in average absorbance between the three campaigns (maximum difference of 15 %). Average absorbance values per campaign, combining all sites, were significantly different (Mann-Whitney test; $p < 0.05$ for campaigns 1 and 2; $p < 0.01$ for campaigns 1 and 3, and 2 and 3).

Fig. 7 shows the difference in average absorbance between the two spatial sources contributing to each confluence, per campaign. For confluences in the northern and central parts of the catchment (Confluences B, C, D, F and K; Fig. 2), samples collected during campaign 1 had the largest difference in average source absorbance (0.082 Abs m^{-1} vs. 0.053 Abs m^{-1} for the other confluences). In contrast, for confluences A and I in the southern part of the catchment, samples collected during campaign 3 showed the highest differences in average source absorbance. For confluences in the northern part of the catchment (Confluences G, J; Fig. 2), samples collected during campaign 3 showed highest differences in average absorbances (0.083 vs 0.045 Abs m^{-1}) compared with other confluences (confluences E and H are discarded as no data were available for campaign 1). For campaign 2, differences
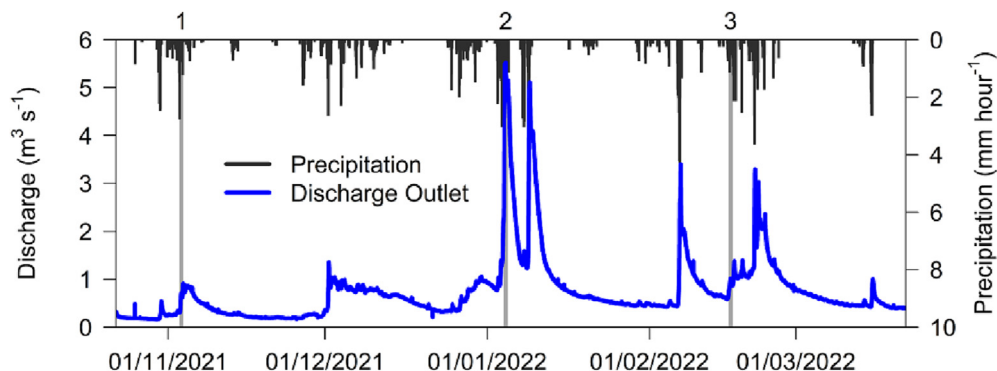
Fig. 4. Precipitation records from the weather station in Reichlange, and measured discharge at the Roudbach catchment outlet in Platen (Fig. 2). The sampling campaigns are highlighted in grey, and indicated by the campaign number (1–3) above the graph.
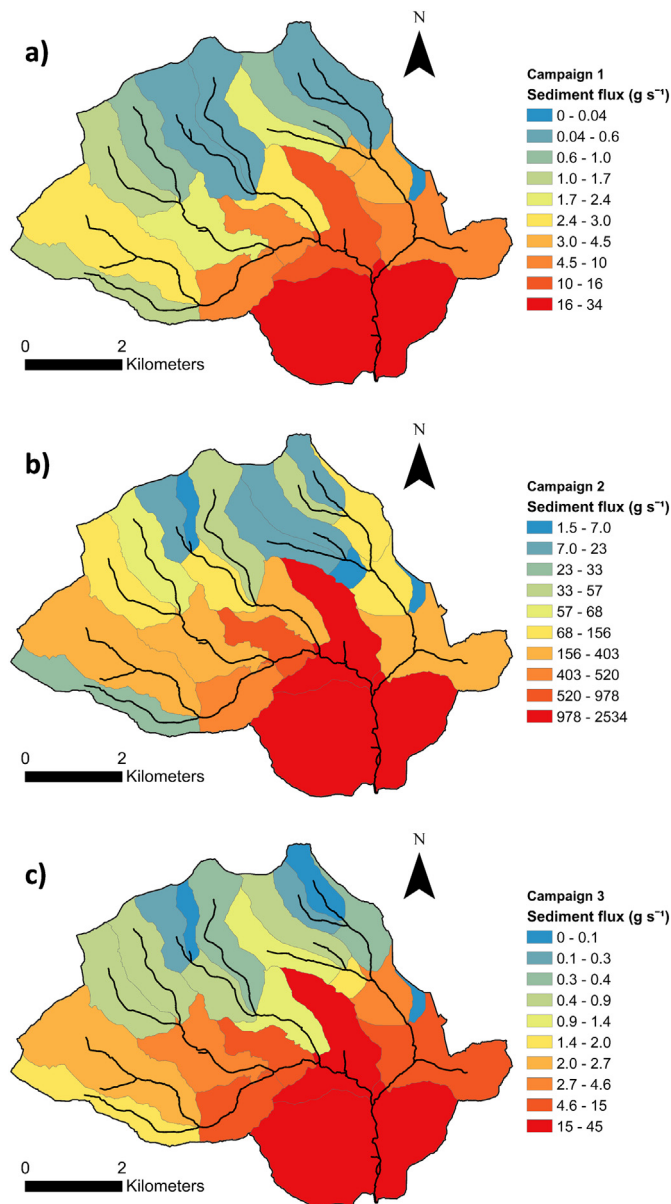
Fig. 5. Spatial overview of suspended sediment (SS) fluxes for the three sampling campaigns in the Roudbach catchment; campaign 1 (a), campaign 2 (b), campaign 3 (c). Areas depicted are the sub-catchments belonging to the different SS spatial source sites (n = 22) for each of the confluences. Colour values represent the different ranges of SS loads, using the Jenks natural breaks classification method applied to 10 intervals (Jenks, 1967).

in source absorbance values were generally lower than during the other campaigns, and none of the confluences in campaign 2 showed differences in source absorbance values being higher than those of campaign 1 or campaign 3. However, for several confluences located in the southern part of the catchment (confluences A, B, C, I and K; Fig. 2) the average source difference (0.052 Abs m^{-1}) during campaign 2 was much higher than in the northern part (confluences E, G, H and J) of the catchment (0.0064 Abs m^{-1}).

Average source absorbance differences were significantly different for all confluences and campaigns (Mann-Whitney test, p < 0.01), except for campaign 1 at confluence F (*p* value = 0.31), campaign 2 at confluence D (*p* value = 0.31) and campaign 3 at confluence B (*p* value = 1.00) where differences between the confluence sources were not statistically different.

3.3. Spatial sediment source fingerprinting: outcomes and evaluation

The average difference ± standard deviation between the source fingerprinting modelling outcomes (Fig. 9; Table S4) and the SS budget estimates (Table 1) for all confluences during the three campaigns was 18 ± 15 %. For individual campaigns, the corresponding average differences were 12 ± 15 %, 20 ± 16 % and 20 ± 12 % for campaign 1, 2 and 3, respectively. The largest differences during campaign 1 were found at confluence K (50 %), during campaign 2 at confluences A, G and J (52, 32 and 38 %, respectively), and during campaign 3 at confluences G and I (48 and 32 %, respectively) (Fig. 8). Deviations between source fingerprinting modelling and the SS budget did not show statistically significant relationships with discharge, SSC or difference in average source absorbance when using the entire dataset (Fig. S1).

From the sediment budget calculations, it was shown that relative contributions of spatial sources at specific confluences varied over the three campaigns; however, at most confluences one of the spatial SS source sites clearly contributes dominant discharge and SS loads. Exceptions in this regard were observed for confluence C and G, which showed a change in the dominant spatial source between campaigns. This change in dominant source was correctly identified by the model for confluence C, but was misclassified by the model for confluence G (Fig. 8). The sediment budgets of confluences A, H, I and K showed relative high variability in relative contributions (≥ 20 %) from same sources over the three campaigns (Table 1). Differences in these source contributions were correctly modelled for confluence H, with absolute deviations between modelling and the SS budget of 1 % (campaign 2) and 4 % (campaign 3). The dominant spatial source at confluence J (campaign 2) and confluence I (campaign 3) was correctly identified by the modelling, but overestimated when compared with the sediment budget (by 38 and 32 % respectively). The sediment budget for confluences A and K showed the same dominant source for the three campaigns. This was not correctly identified by the fingerprinting model for confluence A, campaign 2, as the model identified the incorrect dominant source. For confluence K, the sediment budget indicated that source 30 dominated during the three campaigns whereas the model predicted source 29 contributed more during campaigns 1 and 3 (Fig. 8).

3.4. Spatial sediment source fingerprinting: different modelling approaches

Fig. 9 shows the modelling results for each confluence (A-K) and sampling campaign when using three different methods to select which wavelengths are used as fingerprints (the three methods are described in Section 2.4.3). The three different methods generated similar results. For campaign 1, only confluence A and confluence B showed differences in the dominant contributing SS source. Higher differences in source apportionment (deviation >20 %) between the different methods were observed for confluence A (campaign 2), confluence C (campaign 1 and 3), confluence D (campaign 2) and confluence G (campaign 2). Differences between the methods using all wavelengths in the 200–730 nm range and using all wavelengths in the 390–730 nm range were on average 12.5 % (5.4 % when omitting the above mentioned cases with differences >20 %). Differences between the methods using all wavelengths in the 390–730 nm range and using wavelengths in the 390–730 nm range at intervals of 10 nm were only 1.6 %.

4. Discussion

4.1. Absorbance patterns

Absorbance values differed at the same sampling sites for the different campaigns. The results also indicated that differences between the sampling sites were generally less pronounced for campaign 2, which took place during the event of highest precipitation (Fig. 7). The lower differences could be linked to more constant contributions of certain SS sources during longer duration rainfall events over the catchment (e.g., Walling
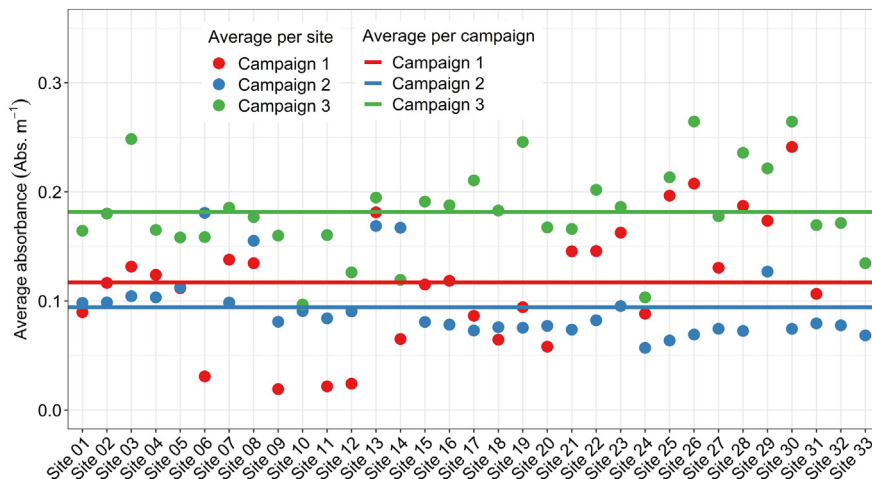
Fig. 6. Average absorbance (represented by circular symbols) for each of the sampling sites, per campaign. The horizontal lines represent the average absorbance of all sampling sites for each campaign.

et al., 2000), thereby indicating the activation of different sources within the spatially defined SS sources areas during the different sampling campaigns (as observed in e.g., Cooper et al., 2015; Cooper et al., 2014; Vercruysse et al., 2017; Vercruysse and Grabowski, 2019). Therefore, the findings of the present study highlight that a single measurement cannot represent the catchment dynamics over time, and thus that methods allowing higher temporal frequency observations are certainly valuable (e.g., Cooper et al., 2015; Pulley and Collins, 2021).

Source absorbance data should be sufficiently different to provide a robust basis for source discrimination and apportionment (Lake et al., 2022a). Herein, absorbance readings for the contributing sources of three confluences did not show significant differences (confluence F in campaign 1, confluence D in campaign 2, and confluence B in campaign 3; Fig. 7). However, these situations did not result in higher deviations in modelled source contributions (Fig. 8) compared with the average deviations for all confluences and campaigns (18 % ± 15). In contrast, confluence K (campaign 1) and confluence G and I (campaign 3) showed very high modelled deviations (respectively 50, 48 and 32 %), even though differences in absorbance for the contributing sources of these confluences were relatively high. This indicates no clear relationship between modelling performance and differences between the absorbance spectra of individual source (Fig. S1).

From the results, it was evident that there is a spatial pattern in absorbance differences between sources merging at different confluences. The main spatial pattern can be found when comparing the average absorbance for the confluences in the northern part of the catchment to those in the southern part. In the northern confluences, there is a relative low difference

between sources (e.g., confluence E and H). This could potentially be explained by the more similar land uses and lithologies in the contributing areas (Fig. 1; Tables S1 and S2). Source streams are thus more likely to transport sediment yielding similar absorbance spectra. With SS source properties influencing absorbance readings (Lake et al., 2022a; Martínez-Carreras et al., 2016; Sehgal et al., 2022), similarity between sources thus provides a limited basis for source discrimination. Nevertheless, similarities in land use and geology do not always seem to explain the small differences in source absorbances for all confluences. Sources at confluence J (Table S1 and S2) are for example largely influenced by the same land use (i.e., forest and cultivated lands) and lithology (i.e., schists, slates and phyllites), but resulted in clearly different absorbance patterns for campaigns 1 and 3 (Fig. 7). These differences could be related to differences in source activations, or a better connectivity of specific sources to the streams under certain conditions (e.g., Fryirs, 2012). The different activation of sources can also be related to one stream (at sampling site 26) starting immediately downstream of a small village, which, upon activation might deliver SS originating from damaged road verges (Collins et al., 2010) and urban sources (Charlesworth and Lees, 2001), thereby affecting the absorbance signal.

4.2. Modelling relative spatial source contributions

This work revealed reasonably small deviations between the spatial source estimates based on sediment fingerprinting and the alternative sediment budgeting approach, with an average deviation for all confluences and campaigns of 18 ± 15 %. The magnitude of deviation was similar to results found by Lake et al. (2022a). Therein, the use of absorbance was evaluated by means of artificial mixtures in a laboratory set-up, reporting errors of 14.5 ± 13 % compared with the known source contributions to artificial mixtures.

There were several instances in which downstream absorbance values did not fall in between the absorbance values from the sources (for all wavelengths). It is common practise in many fingerprinting studies to discard these out of range fingerprints (e.g., Collins et al., 2020; Evrard et al., 2022), due to issues concerning non-conservative behaviour of SS properties. However, this was not deemed necessary in the work reported herein. The distance between the source SS sampling sites and the downstream target SS sampling site was small (20–40 m for confluences E-K, slightly larger for confluences A-D due to field situation/site accessibility). Therefore, logically, it seems unlikely that substantial alterations to SS properties had occurred when SS was transported over such short distances. Furthermore, no clear excessive erosion input was observed at the different confluences in question between the source and target sampling sites. Potential intermediate SS inputs that could have influenced the absorbance measurements were therefore not considered as being of concern.
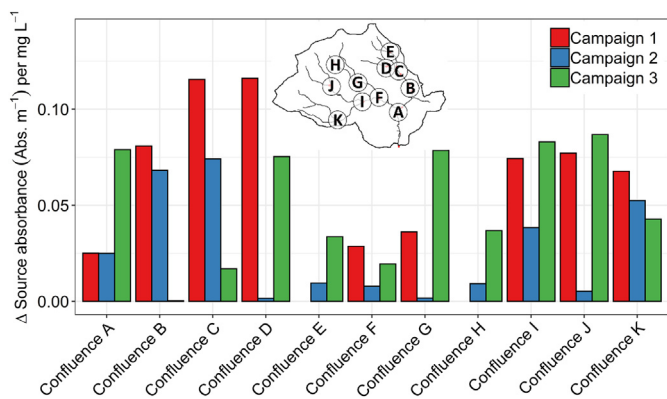
Fig. 7. Mean absorbance differences between the two sources (Δ source absorbance) at each confluence, per campaign. The catchment map locating each confluence (letters A-K) is shown for reference.
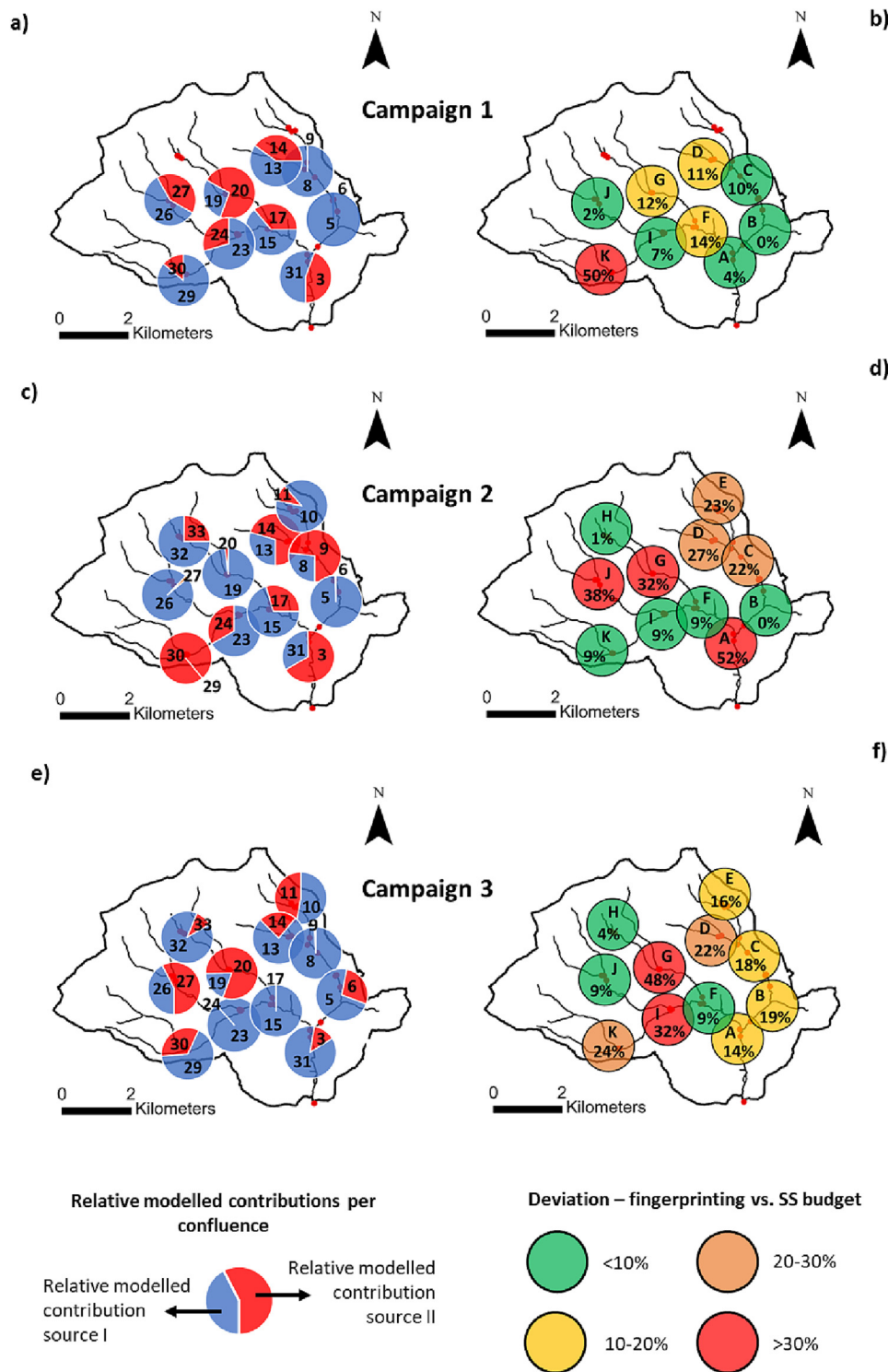
Fig. 8. Relative modelled spatial source contributions for each of the confluences, for sampling campaigns 1 (a), 2 (c) and 3 (e). Modelled source contributions are depicted in the pie-charts. Numbers within the pie-charts indicate the two upstream source sampling sites for each confluence. Percentage of deviation refers to the differences between the fingerprinting and sediment budget, based on relative estimates of source contributions, for sampling campaign 1 (b), 2 (d) and 3 (f). The colour of the confluence circles indicates the extent of deviation between the two approaches.

A more likely explanation for the out of range situations is related to one of the sources being highly dominant. It is expected that the absorbance values of the target SS would then be close to the absorbance values of this dominant source. However, absorbance values of the source and target SS samples are subject to sampling and laboratory measurement uncertainties. Sampling uncertainties include the fact that the grab samples do not fully represent the stream cross-section (e.g., Bainbridge et al., 2012).

Herein, we aimed to take samples from the middle of the cross-section, which was especially challenging in the wider streams. After collection, samples were stored and flocculation might have occurred (Phillips and Walling, 1995), potentially influencing the SS particle size distribution. This, in turn, might have influenced the absorbance readings (Lake et al., 2022a) measured in the laboratory set-up, despite efforts to break-up flocs by shaking the samples and using a magnetic stirrer for sample
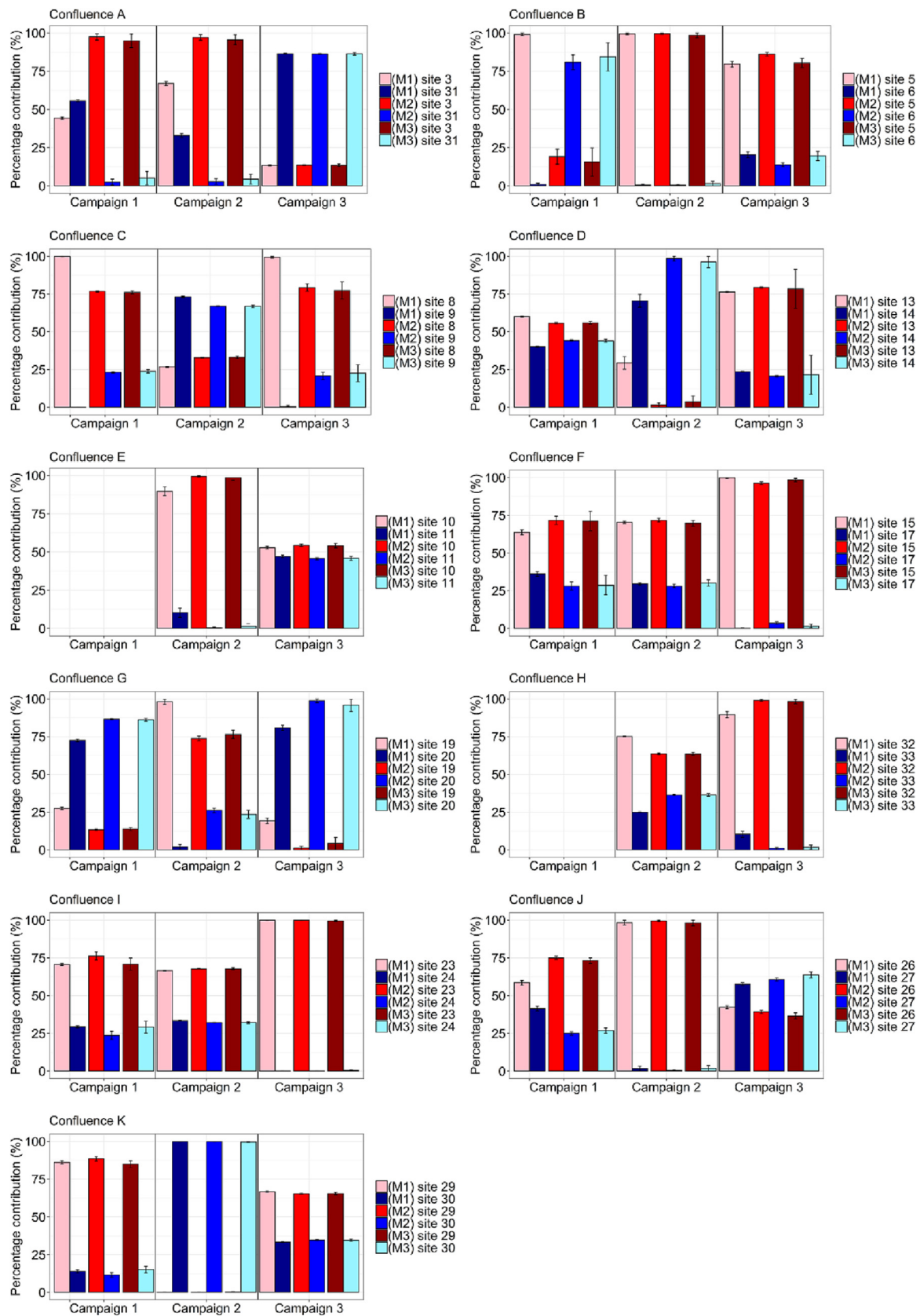
Fig. 9. Modelling results for the sources at all confluences (A-K) for the three measurement campaigns. The results refer to the three different modelling procedures testing three different methods of fingerprint selection using different wavelengths: (M1) using 200–730 nm at 2.5 nm intervals, (M2) using 390–730 nm at 2.5 nm intervals, and (M3) using 390–730 nm at 10 nm intervals. During campaign 1, there was no data for confluences E and H.

resuspension and disaggregation. Furthermore, as absorbance data were compensated for SSC, uncertainty associated with the laboratory methods used to quantify SSC gravimetrically might help explain these out of range situations. Confluences failing the range test do show rather small differences in target SS absorbance compared with the dominant source (with percentage deviations ranging between 3 % and 11 %). These deviations were found to be within reasonable uncertainty ranges for determining SSC (Siu et al., 2008). Therefore, we argue that out of range absorbance situations could still provide valuable information for determining highly dominant source contributions. The latter logic is supported by, for example, Evrard et al. (2022), García-Comendador et al. (2021), Pulley and Collins (2022) who all argue that the identification of dominant SS sources can still be very informative. Similar out of range observations were made by Lake et al. (2022a), resulting in a contribution of ~100 % for the dominant source.

The MixSIAR model (Stock et al., 2018; Stock and Semmens, 2016) was used to apportion the target SS collected downstream at each confluence. Alternatively, a deconvolutional MixSIAR (Blake et al., 2018) model can be applied, which allows accounting for structural hierarchy inside the catchment by progressively applying MixSIAR to downstream confluences. In this case, target SS samples can serve as sources for confluences downstream, thereby reducing the number of samples that need to be collected. In our case, however, the need to apply a deconvolutional MixSIAR approach was negated by the design of our proof-of-concept study.

4.3. Comparison of modelling approaches

In this study, we opted to use all wavelengths (200–730 nm, at 2.5 nm intervals) in the Bayesian modelling framework (MixSIAR) instead of selecting an optimal set of fingerprints through the application of statistical tests (e.g., using a Kruskal-Wallis test combined with a discriminant function analysis) as used in many sediment fingerprinting studies (e.g., Batista et al., 2022; Gaspar et al., 2022; Nosrati et al., 2022). Lake et al. (2022a) obtained accurate results using the same method. This is supported by other studies (e.g., Sherriff et al., 2015), in which it has been suggested that the inclusion of a higher number of fingerprints can improve model performance and decrease the uncertainty associated with the results. Here, the use of all wavelengths over a selected sub-set is also beneficial because it facilitates the implementation of a standardized approach allowing for comparisons between studies (Evrard et al., 2022).

Despite the aforementioned advantages regarding the use of all wavelengths, there are some disadvantages. Using all wavelengths contributes to long model computation times, with collinearity between fingerprints. To account for these issues, two other modelling approaches were tested. The different modelling approaches tested compared well with each other (Fig. 9), with similar modelling outcomes when comparing the 390–730 nm range with the whole range of 200–730 nm (as proposed by Lake et al., 2022a). Limiting the range of wavelengths used has another advantage by removing the need for compensation for the absorbance of background water (i.e., filtered water); dissolved components mainly influence the 200–390 nm range (see Fig. S2, and e.g., Rieger et al., 2004). However, minimal effects of dissolved components were observed for measurements in the 390–730 nm range (Fig. S2). The use of the 390–730 nm range can thus contribute to reducing issues associated with laboratory workload by eliminating the need for filtering and measuring absorbance on filtered water samples.

4.4. Outlook for high spatial and temporal resolution sediment source fingerprinting

Applying the confluence-based approach directly addresses some known challenges associated with sediment fingerprinting, including issues concerning which particle size fraction is being transported from the sources to the channel system. Furthermore, the confluence based approach can provide a better spatial overview of SS origins (Fig. 5), in contrast to most other (i.e., classical) sediment fingerprinting studies which have

aimed to apportion SS contributions based on different land uses (i.e., individual source types). Applying this more classical approach would require the separation of the relevant particle size fractions to create proxy SS soil source samples (e.g., for distinguishing land uses) that can be measured with a submersible spectrophotometer. Exploration of this could be a potential future research topic. Such an approach has the advantage that only one spectrophotometer would be needed at the catchment outlet instead of three spectrophotometers, when measuring in situ, using a confluence-based approach. This would then reduce the initial purchasing costs of the spectrophotometer (~US$20.000 each).

The results obtained using absorbance for tracing SS spatial sources were validated using a sediment budget approach (e.g., Lake et al., 2022b; Tiecher et al., 2022). The need for such independent evaluation when using sediment fingerprinting has been long emphasized (e.g., Collins and Walling, 2004). Estimation of the suspended sediment budget was possible because discharge data were available for some of the sites, permitting calculations of actual SS loads. For the sites where discharge data were not available, the drainage area method was used to estimate discharge (e.g., Emerson et al., 2005). This simple method assumes that discharge is solely a function of catchment area, and will likely introduce uncertainties into the calculations. This is most likely for the sites located higher upstream in the catchment (northern sites), where discharges were low compared with the downstream sites. Despite such uncertainties, the discharge data combined with SSC measurements allowed for an independent evaluation of the contribution of the different SS sources estimated using source fingerprinting, whereas many SS fingerprinting studies do not evaluate predicted source proportions using independent evidence. Instead, an increasing number of recent publications rely on the results of either virtual or artificial mixture tests (e.g., Batista et al., 2022). Although this is an important step in state-of-the-art decision trees for applying sediment source fingerprinting, they have inherent uncertainties and limitations (Collins et al., 2017). Mixtures represent ideal situations (i.e., sources are known, negligible particle size selectivity effects and no out of range fingerprints), meaning that even 'acceptable' modelling results (i.e., modelled results are in agreement with the known proportions in the mixtures) do not always translate into accurate catchment source apportionments (Batista et al., 2022). Clearly, other means to evaluation the un-mixing results using the absorbance data could involve applying more classical sediment fingerprinting approaches and their conventional fingerprint properties.

The approach tested in the present study can facilitate an increase in the temporal resolution of observations for elucidating potential changes in SS source contributions, due to the relatively easy analysis of the water samples. Such information can facilitate the reliable targeting of management solutions to prevent excessive SS transport (e.g., Vercruysse et al., 2017; Vercruysse and Grabowski, 2019). To facilitate an increase in high frequency observations of SS source contributions even further, it is key to reduce sampling and laboratory analyses to a minimum. Here, the use of the absorbance in the 390–730 nm range eliminates the need for compensation for the absorbance of background (filtered) water (i.e., absorbance influenced by dissolved components). This could then allow the direct use of absorbance data collected in situ with a submerged spectrophotometer at high frequency (i.e., minutes) to fingerprint SS sources, further reducing sampling needs and laboratory workloads. Here, the use of in situ absorbance measurements would additionally reduce issues associated with potential alteration of SS properties during transport and storage (Smith and Owens, 2014). Clearly, however, regular sampling to confirm the reliability of the absorbance data would still be needed (Gamerith et al., 2011).

There remains the need to compensate absorbance spectra for SSCs. When using a submerged spectrometer to trace SS sources at high frequency, compensation can be done by establishing a rating curve between SSC and turbidity (the latter also being measured by the spectrophotometer). To this end, a number of grab samples need to be collected and their SSCs need to be measured in the laboratory. Another consideration is the maintenance of the spectrophotometer while installed in situ. The spectrophotometer used in this study can be equipped with an automatic cleaning brush (s::can GmbH, Vienna, Austria) that cleans the sensor lens before

every measurement, to mechanically remove fouling (e.g., Sehgal et al., 2022). Additionally, regular manual cleaning is also advised, e.g., bi-weekly (Martínez-Carreras et al., 2016).

5. Conclusions

In this research, the use of absorbance at a range of wavelengths (i.e., fingerprints) to apportion SS spatial source contributions using a confluence-based sampling strategy was tested. This new research builds upon the work presented by Lake et al. (2022a), who tested and evaluated the absorbance approach in a laboratory setting using artificially created source samples and mixtures. The results presented herein suggested that confluences in the northern part of the study catchment exhibited lower differences between source absorbance compared with confluences in the southern part, indicating the potential influence of different spatial sources. Absorbance measured at the same sampling sites varied over time, indicating the need for repeat sampling if catchment SS dynamics are to be well understood. Modelled SS spatial source contributions showed deviations of 18 ± 15 % from the corresponding source contributions estimated using sediment budgets. While dominant spatial sources were mostly well identified using the absorbance fingerprinting approach, some clear deviations from the budget approach were observed. Care is thus needed when using absorbance for fingerprinting and independent evaluation of the results should be undertaken on a regular basis.

There were no clear indications of improved model performances with higher source absorbance differences, increasing discharges or higher SSCs. Furthermore, it was shown that different modelling procedures gave comparable spatial source estimates. Hence, computation times could be reduced by using a lower number of wavelengths as fingerprints. Overall, this research has shown that, despite some uncertainties in the modelling results, absorbance could potentially be used as a sediment fingerprint in natural environments, reducing the need for conventional resource intensive laboratory preparation and analyses of source and target SS samples. The method reported herein, using a submerged spectrophotometer, could thus contribute to easier ways of estimating SS source contributions and such information is urgently needed to improve the targeting of sediment control strategies in many river catchments.

CRediT authorship contribution statement

Niels F. Lake: Conceptualisation, Methodology, Formal analysis, Investigation, Resources, Visualisation, Writing – original draft. **Núria Martínez-Carreras:** Funding acquisition, Conceptualisation, Methodology, Resources, Supervision, Writing – review & editing. **Peter J. Shaw:** Conceptualisation, Methodology, Supervision, Writing – review & editing. **Jean-François Iffly:** Conceptualization, Methodology, Resources. **Adrian L. Collins:** Conceptualisation, Methodology, Supervision, Writing – review & editing.

Data availability

Precipitation records from the weather station at Reichlange (see Fig. 1b,c) were made available by the 'Administration de la Gestion de l'Eau' (AGE; https://www.agrimeteo.lu). Land use, lithology and elevation data is made available by the 'Administration du Cadastre et de la Topographie' (ACT; https://map.geoportail.lu). Absorbance data measured on the water samples collected in all sampling sites, for the three campaigns, is available at zenodo.org (Lake and Martínez-Carreras 2023, https://doi.org/10.5281/zenodo.7664171). For more information please contact the authors (Niels Lake, niels-lake3@hotmail.com; Núria Martínez-Carreras, nuria.martinez@list.lu.

Declaration of competing interest

The authors declare that they have no known competing financial interests or personal relationships that could have appeared to influence the work reported in this paper.

Appendix A. Supplementary data

Supplementary data to this article can be found online at https://doi.org/10.1016/j.scitotenv.2023.162332.

References

Bainbridge, Z.T., Wolanski, E., Álvarez-Romero, J.G., Lewis, S.E., Brodie, J.E., 2012. Fine sediment and nutrient dynamics related to particle size and floc formation in a Burdekin River flood plume,Australia. Mar. Pollut. Bull. 65, 236–248. https://doi.org/10.1016/j.marpolbul.2012.01.043.

Batista, P.V.G., Laceby, J.P., Evrard, O., 2022. How to evaluate sediment fingerprinting source apportionments. J. Soils Sediments https://doi.org/10.1007/s11368-022-03157-4.

Blake, W.H., Boeckx, P., Stock, B.C., Smith, H.G., Bodé, S., Upadhayay, H.R., Gaspar, L., Goddard, R., Lennard, A.T., Lizaga, I., Lobb, D.A., Owens, P.N., Petticrew, E.L., Kuzyk, Z.Z.A., Gari, B.D., Munishi, L., Mtei, K., Nebiyu, A., Mabit, L., Navas, A., Semmens, B.X., 2018. A deconvolutional Bayesian mixing model approach for river basin sediment source apportionment. Sci. Rep. 8, 1–12. https://doi.org/10.1038/s41598-018-30905-9.

Borrelli, P., Robinson, D.A., Fleischer, L.R., Lugato, E., Ballabio, C., Alewell, C., Meusburger, K., Modugno, S., Schütt, B., Ferro, V., Bagarello, V., Oost, K.Van, Montanarella, L., Panagos, P., 2017. An assessment of the global impact of 21st century land use change on soil erosion. Nat. Commun. 8. https://doi.org/10.1038/s41467-017-02142-7.

Byrne, A.J., Chow, C., Trolio, R., Lethorn, A., Lucas, J., Korshin, G.V., 2011. Development and validation of online surrogate parameters for water quality monitoring at a conventional water treatment plant using a UV absorbance spectrolyser. Proc. 2011 7th Int. Conf. Intell. Sensors, Sens. Networks Inf. Process. ISSNIP 2011, pp. 200–204 https://doi.org/10.1109/ISSNIP.2011.6146515.

Charlesworth, S.M., Lees, J.A., 2001. The application of some mineral magnetic measurements and heavy metal analysis for characterising fine sediments in an urban catchment, Coventry, UK. J. Appl. Geophys. 48, 113–125. https://doi.org/10.1016/S0926-9851(01)00084-2.

Collins, A.L., Blackwell, M., Boeckx, P., Chivers, C.A., Emelko, M., Evrard, O., Foster, I., Gellis, A., Gholami, H., Granger, S., Harris, P., Horowitz, A.J., Laceby, J.P., Martinez-Carreras, N., Minella, J., Mol, L., Nosrati, K., Pulley, S., Silins, U., da Silva, Y.J., Stone, M., Tiecher, T., Upadhayay, H.R., Zhang, Y., 2020. Sediment source fingerprinting: benchmarking recent outputs, remaining challenges and emerging themes. J. Soils Sediments 20, 4160–4193. https://doi.org/10.1007/s11368-020-02755-4.

Collins, A.L., Pulley, S., Foster, I.D.L., Gellis, A., Porto, P., Horowitz, A.J., 2017. Sediment source fingerprinting as an aid to catchment management: a review of the current state of knowledge and a methodological decision-tree for end-users. J. Environ. Manag. 194, 86–108. https://doi.org/10.1016/j.jenvman.2016.09.075.

Collins, A.L., Walling, D., Leeks, G.J.L., 1996. Composite fingerprinting of the spatial source of fluvial suspended sediment: a case study of the Exe and Severn river basins, United Kingdom. Géomorphol. Relief Process. Environ. 2, 41–53. https://doi.org/10.3406/morfo.1996.877.

Collins, A.L., Walling, D.E., 2004. Documenting catchment suspended sediment sources: problems, approaches and prospects. Prog. Phys. Geogr. Earth Environ. 28, 159–196. https://doi.org/10.1191/0309133304 pp409ra.

Collins, A.L., Walling, D.E., Leeks, G.J.L., 1997. Fingerprinting the origin of fluvial suspended sediment in larger river basins: combining assessment of spatial provenance and source type. Geogr. Ann. Ser. A Phys. Geogr. 79, 239–254. https://doi.org/10.1111/j.0435-3676.1997.00020.x.

Collins, A.L., Walling, D.E., Stroud, R.W., Robson, M., Peet, L.M., 2010. Assessing damaged road verges as a suspended sediment source in the Hampshire Avon catchment, southern United Kingdom. Hydrol. Process. 24, 1106–1122. https://doi.org/10.1002/hyp.7573.

Cooper, R.J., Krueger, T., Hiscock, K.M., Rawlins, B.G., 2015. High-temporal resolution fluvial sediment source fingerprinting with uncertainy: a Bayesian approach. Earth Surf. Process. Landforms 40, 78–92. https://doi.org/10.1002/esp.3621.

Cooper, R.J., Rawlins, B.G., Lézé, B., Krueger, T., Hiscock, K.M., 2014. Combining two filter paper-based analytical methods to monitor temporal variations in the geochemical properties of fluvial suspended particulate matter. Hydrol. Process. 28, 4042–4056. https://doi.org/10.1002/hyp.9945.

Emerson, D.G., Vecchia, A.V., Dahl, A.L., 2005. Evaluation of drainage-area ratio method used to estimate streamflow for the Red river of the north basin, North Dakota and Minnesota. US Geol. Surv. Sci. Investig. Rep.

Evrard, O., Batista, P.V.G., Company, J., Dabrin, A., Foucher, A., Frankl, A., García-Comendador, J., Huguet, A., Lake, N., Lizaga, I., Martínez-Carreras, N., Navratil, O., Pignol, C., Sellier, V., 2022. Improving the design and implementation of sediment fingerprinting studies: summary and outcomes of the TRACING 2021 Scientific School. J. Soils Sediments 22, 1648–1661. https://doi.org/10.1007/s11368-022-03203-1.

Fryirs, K., 2012. (Dis) connectivity in catchment sediment cascades: a fresh look at the sediment delivery problem. Earth Surf. Process. Landforms 38, 30–46. https://doi.org/10.1002/esp.3242.

Gamerith, V., Steger, B., Hochedlinger, M., Gruber, G., 2011. Assessment of UV/VIS-spectrometry performance in combined sewer monitoring under wet weather conditions. 12th Int. Conf. Urban Drainage, Porto Alegre/Brazil, pp. 10–15.

García-Comendador, J., Martínez-Carreras, N., Fortesa, J., Company, J., Borràs, A., Estrany, J., 2021. Combining sediment fingerprinting and hydro-sedimentary monitoring to assess suspended sediment provenance in a mid-mountainous Mediterranean catchment. J. Environ. Manag. 299, 113593. https://doi.org/10.1016/j.jenvman.2021.113593.

Gaspar, L., Blake, W.H., Lizaga, I., Latorre, B., Navas, A., 2022. Particle size effect on geochemical composition of experimental soil mixtures relevant for unmixing modelling. Geomorphology 403, 108178. https://doi.org/10.1016/j.geomorph.2022.108178.

Jenks, G.F., 1967. The data model concept in statistical mapping. Int. Yearb. Cartogr. 7, pp. 186–190.

Klages, M.G., Hsieh, Y.P., 1975. Suspended solids carried by the Gallatin River of southwestern Montana: II. Using mineralogy for inferring sources. J. Environ. Qual. 4, 68–73. https://doi.org/10.2134/jeq1975.00472425000400010006x.

Laceby, J.P., Evrard, O., Smith, H.G., Blake, W.H., Olley, J.M., Minella, J.P.G., Owens, P.N., 2017. The challenges and opportunities of addressing particle size effects in sediment source fingerprinting: a review. Earth-Sci.Rev. 169, 85–103. https://doi.org/10.1016/j.earscirev.2017.04.009.

Lake, N.F., Martínez-Carreras, N., Shaw, P.J., Collins, A.L., 2022a. High frequency un-mixing of soil samples using a submerged spectrophotometer in a laboratory setting—implications for sediment fingerprinting. J. Soils Sediments 22, 348–364. https://doi.org/10.1007/s11368-021-03107-6.

Lake, N.F., Martínez-Carreras, N., Shaw, P.J., Collins, A.L., 2022b. Using particle size distributions to fingerprint suspended sediment sources — evaluation at laboratory and catchment scales. Hydrol. Process. 36, e14726. https://doi.org/10.1002/hyp.14726.

Lake, N.F., Martínez-Carreras, N., 2023. Data to reproduce the results presented in Lake et al. 2023. Sci. Total Environ. https://doi.org/10.1016/j.scitotenv.2023.162332 ("Use of a submersible spectrophotometer probe to fingerprint spatial suspended sediment sources at catchment scale"). Zenodo, Version 1, https://doi.org/10.5281/zenodo.7664171.

Legout, C., Poulenard, J., Nemery, J., Navratil, O., Grangeon, T., Evrard, O., Esteves, M., 2013. Quantifying suspended sediment sources during runoff events in headwater catchments using spectrocolorimetry. J. Soils Sediments 13, 1478–1492. https://doi.org/10.1007/s11368-013-0728-9.

Martínez-Carreras, N., Krein, A., Udelhoven, T., Gallart, F., Iffly, J.F., Hoffmann, L., Pfister, L., Walling, D.E., 2010a. A rapid spectral-reflectance-based fingerprinting approach for documenting suspended sediment sources during storm runoff events. J. Soils Sediments 10, 400–413. https://doi.org/10.1007/s11368-009-0162-1.

Martínez-Carreras, N., Schwab, M.P., Klaus, J., Hissler, C., 2016. In situ and high frequency monitoring of suspended sediment properties using a spectrophotometric sensor. Hydrol. Process. 30, 3533–3540. https://doi.org/10.1002/hyp.10858.

Martínez-Carreras, N., Udelhoven, T., Krein, A., Gallart, F., Iffly, J.F., Ziebel, J., Hoffmann, L., Pfister, L., Walling, D.E., 2010b. The use of sediment colour measured by diffuse reflectance spectrometry to determine sediment sources: application to the Attert River catchment (Luxembourg). J. Hydrol. 382, 49–63. https://doi.org/10.1016/j.jhydrol.2009.12.017.

Navratil, O., Evrard, O., Esteves, M., Legout, C., Ayrault, S., Némery, J., Mate-Marin, A., Ahmadi, M., Lefèvre, I., Poirel, A., Bonté, P., 2012. Temporal variability of suspended sediment sources in an alpine catchment combining river/rainfall monitoring and sediment fingerprinting. Earth Surf. Process. Landforms 37, 828–846. https://doi.org/10.1002/esp.3201.

Nones, M., 2019. Dealing with sediment transport in flood risk management. Acta Geophys. 67, 677–685. https://doi.org/10.1007/s11600-019-00273-7.

Nosrati, K., Moradian, H., Dolatkordestani, M., Mol, L., Collins, A.L., 2022. The efficiency of elemental geochemistry and weathering indices as tracers in aeolian sediment provenance fingerprinting. Catena 210, 105932. https://doi.org/10.1016/j.catena.2021.105932.

Owens, P.N., Batalla, R.J., Collins, A.J., Gomez, B., Hicks, D.M., Horowitz, A.J., Kondolf, G.M., Marden, M., Page, M.J., Peacock, D.H., Petticrew, E.L., Salomons, W., Trustrum, N.A.,

2005. Fine-grained sediment in river systems: environmental significance and management issues. River Res. Appl. 21, 693–717. https://doi.org/10.1002/rra.878.

Owens, P.N., Petticrew, E.L., van der Perk, M., 2010. Sediment response to catchment disturbances. J. Soils Sediments 10, 591–596. https://doi.org/10.1007/s11368-010-0235-1.

Pfister, L., Wagner, C., Vansuypeene, E., Drogue, G., Hoffmann, L., Ries, C., 2005. Atlas Climatique du Grand-Duché de Luxembourg. Musée National d'Histoire Naturelle, Société des Naturalistes Luxembourgeois, Centre de Recherce Public-Gabriel Lippmann, Administration des Services Techniques de l'Agriculture, Luxembourg 80 p.

Phillips, J.M., Walling, D.E., 1995. An assessment of the effects of sample collection, storage and resuspension on the representativeness of measurements of the effective particle size of fluvial suspended sediment. Water Res. 29, 2498–2508.

Pulley, S., Collins, A.L., 2022. A rapid and inexpensive colour-based sediment tracing method incorporating hydrogen peroxide sample treatment as an alternative to quantitative source fingerprinting for catchment management. J. Environ. Manag. 311, 114780. https://doi.org/10.1016/j.jenvman.2022.114780.

Pulley, S., Collins, A.L., 2021. The potential for colour to provide a robust alternative to high-cost sediment source fingerprinting: assessment using eight catchments in England. Sci. Total Environ. 792, 148416. https://doi.org/10.1016/j.scitotenv.2021.148416.

Pulley, S., Rowntree, K., 2016. The use of an ordinary colour scanner to fingerprint sediment sources in the South African Karoo. J. Environ. Manag. 165, 253–262. https://doi.org/10.1016/j.jenvman.2015.09.037.

Rieger, L., Langergraber, G., Thomann, M., Fleischmann, N., Siegrist, H., 2004. Spectral in-situ analysis of NO2, NO3, COD, DOC and TSS in the effluent of a WWTP. Water Sci. Technol. 50, 143–152. https://doi.org/10.2166/wst.2004.0682.

Sehgal, D., Martínez-Carreras, N., Hissler, C., Bense, V.F., Hoitink, A.J.F.(Ton), 2022. Inferring suspended sediment carbon content and particle size at high-frequency from the optical response of a submerged spectrometer. Water Resour. Res. 58, e2021WR030624. https://doi.org/10.1029/2021wr030624.

Sherriff, S.C., Franks, S.W., Rowan, J.S., Fenton, O., Ó'hUallacháin, D., 2015. Uncertainty-based assessment of tracer selection, tracer non-conservativeness and multiple solutions in sediment fingerprinting using synthetic and field data. J. Soils Sediments 15, 2101–2116. https://doi.org/10.1007/s11368-015-1123-5.

Siu, C.Y.S., Pitt, R., Clark, S.E., 2008. Errors associated with sampling and measurement of solids: application to the evaluation of stormwater treatment devices. CD-ROM Proceedings of the 11th Int. Conf. on Urban Drainage, Edinburgh, UK, pp. 1–10.

Smith, T.B., Owens, P.N., 2014. Flume- and field-based evaluation of a time-integrated suspended sediment sampler for the analysis of sediment properties. Earth Surf. Process. Landforms 39, 1197–1207. https://doi.org/10.1002/esp.3528.

Stock, B.C., Jackson, A.L., Ward, E.J., Parnell, A.C., Phillips, D.L., Semmens, B.X., 2018. Analyzing mixing systems using a new generation of Bayesian tracer mixing models. PeerJ 2018, 1–27. https://doi.org/10.7717/peerj.5096.

Stock, B.C., Semmens, B.X., 2016. MixSIAR GUI User Manual. Version 3.1.Available at https://github.com/brianstock/MixSIAR (Accessed November 2022).

Tiecher, T., Ramon, R., de Andrade, L.C., Camargo, F.A.O., Evrard, O., Minella, J.P.G., Laceby, J.P., Bortoluzzi, E.C., Merten, G.H., Rheinheimer, D.S., Walling, D.E., Barros, C.A.P., 2022. Tributary contributions to sediment deposited in the Jacuí Delta,Southern Brazil. J. Great Lakes Res. 48, 669–685. https://doi.org/10.1016/j.jglr.2022.02.006.

Vercruysse, K., Grabowski, R.C., 2019. Temporal variation in suspended sediment transport: linking sediment sources and hydro-meteorological drivers. Earth Surf. Process. Landforms 44, 2587–2599. https://doi.org/10.1002/esp.4682.

Vercruysse, K., Grabowski, R.C., Rickson, R.J., 2017. Suspended sediment transport dynamics in rivers: multi-scale drivers of temporal variation. Earth-Sci.Rev. 166, 38–52. https://doi.org/10.1016/j.earscirev.2016.12.016.

Walling, D.E., Owens, P.N., Waterfall, B.D., Leeks, G.J.L., Wass, P.D., 2000. The particle size characteristics of fluvial suspended sediment in the humber and tweed catchments,UK. Sci. Total Environ. 251–252, 205–222. https://doi.org/10.1016/S0048-9697(00)00384-3.

WFD, 2000/60/EC, 2000. Directive 2000/60/EC of the European Parliament and the Council of 23.10.2000, A framework for community action in the field of water policy. Off. J. Eur. Communities 71.